X-RAY MEASUREMENT OF RESIDUAL STRESSES IN TITANIUM ALLOY SHEET

By David N. Braski and Dick M. Royster

NASA Langley Research Center
Langley Station, Hampton, Va.

Presented at the 15th Annual Conference on
Applications of X-Ray Analysis

Denver, Colorado
August 10-12, 1966

X-RAY MEASUREMENT OF RESIDUAL STRESSES IN TITANIUM ALLOY SHEET

By David N. Braski and Dick M. Royster

NASA Langley Research Center

SUMMARY

An X-ray diffraction technique was used to measure residual stresses in Ti-6Al-4V and Ti-8Al-1Mo-1V sheet created by glass-bead peening, sand and aluminum oxide blasting, and a vibratory tumbling treatment. For peening and blasting, the use of larger particle sizes produced greater compressive stresses. In the case of the vibratory treatment, an increase in vibratory frequency or treatment time increased the compressive stress. Glass-bead peening caused a 10-percent reduction in yield strength while the other treatments had little effect on the tensile properties. Significant stress relaxation occurred in all the treated Ti-6Al-4V coupons exposed at 600° F and 800° F.

INTRODUCTION

The concept of inducing residual compressive stresses in a metal alloy for the prevention of stress corrosion is generally well known. (See, for example, ref. 1.) Recent studies at the NASA Langley Research Center which have utilized this concept indicate that certain surface treatments will protect titanium alloys against salt-stress corrosion at temperatures below 600° F. (See refs. 2 and 3.) Other research at Langley has been aimed at alleviating the stress corrosion of Ti-6Al-4V in nitrogen tetroxide by glass-bead peening the exposed surfaces. However, the use of surface treatments on titanium alloys has raised questions in regard to the magnitude and distribution of residual compressive stresses that are created.

In this investigation residual surface stresses produced in Ti-6Al-4V and Ti-8Al-1Mo-1V sheet by glass-bead peening, sand and aluminum oxide blasting, and a vibratory tumbling process have been determined by X-ray diffraction. The analysis was facilitated by use of a high-speed digital computer. The distribution of residual compressive stresses was determined by chemically milling off thin layers of material and taking X-ray measurements. Treatment parameters such as particle size and treatment time were varied to study their effect on the magnitude and distribution of residual stresses. The effect of exposure in the temperature range from room temperature to 800° F on the residual stresses and the effect of surface treatment on tensile properties were also investigated. Light and electron microscopy, as well as surface roughness measurements, were used to study surface characteristics produced by the different treatments.

PROCEDURE

Material

The materials used in this investigation were 0.046-inch-thick Ti-6Al-4V and 0.050-inch-thick Ti-8Al-1Mo-1V sheet in the annealed and duplex annealed heat-treated conditions, respectively. The chemical composition of each alloy in percent by weight, as supplied by the producer, is as follows:

Alloy	C	Fe	N	Al	V	Mo	H	Ti
Ti-6Al-4V	0.023	0.1	0.01	5.9	4.1	---	0.007	Balance
Ti-8Al-1Mo-1V	.026	.08	.012	7.8	1.0	1.0	.006	Balance

Specimen Preparation

The specimens were fabricated by first shearing the sheet into $1\frac{1}{2}$-inch by $1\frac{1}{2}$-inch coupons. The coupons were then glass-bead peened, blasted, or given a vibratory treatment by using the treatment parameters listed in table I. Table I also lists the commercial designation, particle composition, and particle size in microns (μ) for each treatment.

Glass-bead peening and blasting were accomplished manually on one side of each coupon by using a nozzle-to-specimen distance of approximately 6 inches. The vibratory-tumbling treatment is a commercial cleaning and deburring process in which the specimens were vibrated in a bath containing aluminum oxide triangles (5/8-inch on each side by 1/4-inch thick) and a detergent. Both faces of the coupons were therefore affected by the vibratory treatment. Several specimens were treated on one side by spotwelding two coupons together at the corners. After treatment the coupons were separated and used for stress-distribution determinations. Vibrational frequencies of 1375 and 1750 cpm were used to vary the degree of tumbling action.

Specimens representative of each treatment were selected for measurement of residual stresses through the treated surface layers and were lacquered on the untreated face. X-ray measurements were then taken on the treated surface and also below the surface in 0.0001-inch increments until the residual stress was zero. The layers of material were removed by chemical milling with a solution consisting of 65cc H_2O, 25cc HNO_3 (conc), and 8cc HF (45% conc). Milling times varied from 3 to 30 seconds, depending on the strength of the solution. The amount of material removed was monitored by taking thickness measurements near each corner and at the center of the coupons with a micrometer.

Surface Examination

In order to gain insight on how the various treatments affect the surface, light and electron photomicrographs were made on both untreated and treated Ti-6Al-4V coupons. The electron micrographs were made by using two-stage plastic-carbon replicas shadowed at 45° with chromium. Surface-roughness measurements were obtained with a commercial profilometer which employed a 0.0005-inch-radius diamond-tipped exploring stylus. Root-mean-square (RMS) values of surface roughness were obtained directly in microinches.

Tensile Tests

To determine the effect of the surface treatments on the tensile properties of Ti-6Al-4V and Ti-8Al-1Mo-1V, a series of ASTM standard tensile specimens were fabricated and given the surface treatments listed in table II. The tensile specimens were treated on both flat surfaces, as well as on the edges of the reduced section. The tensile tests were performed in a 100-kip hydraulic testing machine.

During the tests the load was recorded autographically against strain. Strain was measured over a 1-inch gage length by means of two linear variable differential transformers attached to the faces of the specimens.

Stress Relaxation Tests

In order to determine the effects of elevated-temperature exposure on the residual stress produced by three representative treatments, single coupons of each treatment were exposed at room temperature, 200° F, 400° F, 600° F, and 800° F for 1000 hours. The 425μ glass-bead-peening, 75μ sand-blasting, and 1750-cpm-vibratory treatments were selected as being typical

and also because they produced substantial residual compressive stresses. The residual surface stress was determined for each specimen at room temperature before exposure and also at selected times throughout the exposure period.

X-Ray Stress Measurements

In the two-exposure X-ray diffraction technique, stresses are obtained by measuring elastic strains associated with a selected set of crystallographic planes. This technique, which is described fully in reference 4, utilizes the following expression:

$$\sigma = K\left(2\theta_0 - 2\theta_\psi\right) \tag{1}$$

where

σ residual surface stress

K stress factor (determined experimentally)

$2\theta_0$ position of selected peak with specimen in normal position

$2\theta_\psi$ position of selected peak with specimen at angle ψ relative to normal position; $\psi = 45^\circ$ for this study.

The three-point parabola method for determining peak position (ref. 4) was used on the reflection from favorably oriented (213) planes. A General Electric XRD-5 diffractometer using nickel-filtered copper K_α radiation at 45 kV and 16 mA was used with a 3° medium-resolution soller slit and a 0.2° detector slit. The (213) reflection was first scanned at 2° per minute to locate the approximate position of the peak and to enable the selection of three suitable points at which to count intensity. The three points were selected above 75 percent of the maximum intensity in order to minimize errors due to peak shape.

The interval selected between points varied from 0.1 to 0.8 degrees depending on the amount of line broadening. Pulse height discrimination was utilized to obtain peak-to-background ratios of at least 3:1. Intensity was measured as reciprocal intensity by recording the time for 40,000 counts. A preset count of 100,000 was used for some subsurface measurements of stress at a time when the pulse height discriminator was malfunctioning. Results of these latter measurements were comparable to those made by using pulse height discrimination because the peaks obtained in subsurface measurements were relatively sharp.

In order to achieve a reasonable degree of accuracy in the X-ray measurement of stress, it was necessary to take into account certain correction factors. The Lorentz polarization and absorption factors taken from reference 4 were applied to the values of reciprocal intensity. Corrections for X-ray beam penetration and for stress relaxation created by the removal of layers were also applied to stress measurements made beneath the surface. The details of these correction factors are described in reference 4.

Stress-Factor Calibration

In this investigation the stress factor K (see eq. (1)) was obtained by measuring the peak shift $(2\theta_0 - 2\theta_{45})$ with the X-ray diffractometer on 6-inch by 5/8-inch strips of each alloy bent around dies of different radii. The tensile strain in the outer fibers of each strip was measured with a strain gage. The X-ray measurement was taken directly adjacent to the strain gage. Young's modulus was used to convert the strain-gage values of strain to stress. Young's modulus was determined for the Ti-6Al-4V and Ti-8Al-1Mo-1V sheet by using standard ASTM tensile specimens of each alloy and Tuckerman optical strain gages.

Computer Program

A computer program used to convert the X-ray data into residual stress values is shown schematically in figure 1. First, the values of reciprocal intensity counted with $\psi = 0^\circ$ and $\psi = 45^\circ$ were fed into the program and corrected by the Lorentz polarization and absorption factors. Then parabolas were fitted to the corrected intensity points to determine the peak positions $2\theta_0$ and $2\theta_{45}$. The peak shift was multiplied by the stress factor to obtain the residual stress. Both $2\theta_0$ and $2\theta_{45}$, along with the surface stress, were printed out by the computer. When surface layers were removed from the coupons, two additional corrections were applied: the beam-penetration correction and the subsurface correction. Because of the variation in the shape of stress profiles, it was believed that more reliable results could be obtained by using the computer to calculate only part of the beam-penetration correction. The portion of this correction which called for slopes on curves of $2\theta_0$ and $2\theta_{45}$ plotted against depth (see ref. 4) was carried out manually and then fed into the computer. Finally, the stress, after all corrections were made, was printed out by the computer.

RESULTS AND DISCUSSION

Stress-Factor Calibration

The results of the calibration to obtain stress factors for Ti-6Al-4V and Ti-8Al-1Mo-1V are shown in figure 2. The stress computed from the strain-gage readings is plotted against the peak shift or $(2\theta_0 - 2\theta_{45})$ measured by X-ray diffraction. Straight lines were fitted to the data points by the method of least squares and displayed slopes or stress factors of 80 and 86 ksi per degree of peak shift for Ti-6Al-4V and Ti-8Al-1Mo-1V, respectively.

Effect of Treatment Parameters on Residual Surface Stress

The results of the stress measurements on Ti-6Al-4V and Ti-8Al-1Mo-1V sheet indicated that the variation in surface stresses produced by the treatments was small enough to permit a meaningful analysis by X-ray diffraction. This is demonstrated in figure 3 for glass-bead peening with 425μ beads after 2- and 10-second treatment times. Five stress measurements were taken on the first specimen in each group and three measurements were taken on the remaining two specimens. The residual-stress value in the figure appears in the area in which it was measured. It is seen that the range of average residual stresses from specimen to specimen was from 2 to 5 ksi. The range of variations of single stresses measured across any one specimen was within 1 to 8 ksi of the average surface stress. It should be pointed out that the surface stress as measured by X-ray diffraction is itself an average of stresses through a thin layer of material. The thickness of the layer is largely dependent on the type of X-ray radiation used.

The effects of varying different treatment parameters on the residual surface stress is shown in figure 4 where residual stress is plotted against treatment time. Each data point is the average of three stress measurements taken on different areas of the same specimen.

The results for glass-bead peening (fig. 4(a)) indicate that, for the ranges investigated, treatment time or bead size had little effect on the magnitude of the residual compressive stress at the surface. However, subsurface stress measurements discussed subsequently show that glass-bead size did have an effect on residual stress. Residual-stress measurements on coupons having sand or aluminum oxide treatments (fig. 4(b)) indicated that increased treatment times caused slight increases in residual compressive

stress. Figure 4(b) also shows that the larger the particle size, the greater the residual compressive stress. For the vibratory treatment on both faces of coupons (fig. 4(c)), increased treatment times produced increases in residual stress in Ti-6Al-4V while little change was noted for Ti-8Al-1Mo-1V. Frequency had a noticeable effect on residual stress as larger residual stresses were produced at 1750 cpm. Note that for the same frequency and shorter treatment times, higher stresses were produced in Ti-8Al-1Mo-1V than Ti-6Al-4V.

Surface Examination

Light and electron photomicrographs of the surface of Ti-6Al-4V coupons before treatment and after glass-bead peening, blasting, and vibratory treatments are given in figures 5 to 8. Figure 5 illustrates the dimpled appearance of the as-received Ti-6Al-4V sheet material at low and high magnification. Several beta platelets are visible in electron micrograph (fig. 5(b)). Figure 6 shows the surface after glass-bead peening with 425μ beads for 5 seconds. Relatively large craters are evident as would be expected from the large glass beads. High magnification (fig. 6(b)) reveals the presence of many slip lines characteristic of rather severe plastic deformation. Figure 7 shows the surface of a coupon which was blasted with 200μ aluminum oxide for 5 seconds. As might be expected from the shape of the particles this treatment produces sharper or more angular irregularities than peening. The effect of a 26-hour vibratory treatment at 1375 cycles/min on the surface is shown in figure 8. Both micrographs clearly show the scratches produced by the aluminum oxide triangles in the vibratory treatment.

Figure 9 shows the results of surface-roughness measurements conducted on glass-bead peened and blasted coupons. Surface roughness in root-mean-square (RMS) is plotted against average particle size in microns. Each symbol represents an average of RMS values obtained for the three data points for each treatment. The range of values is given by the bars through each point. The RMS value for the untreated material is plotted on the ordinate. The surface-roughness measurements indicated that the larger the particle size, the rougher the surface finish. On the other hand, treatment time in the range investigated had little effect on surface roughness. The vibratory treatment produced RMS values of approximately 7 micro-inches, which was essentially the same as those for untreated material.

Subsurface Stress Measurements

The results of stress measurements conducted beneath the surface of coupons are presented in figures 10, 11, and 12. Measurements of residual stress were made in depth increments of 0.0001 inch. The resulting stress-distribution curves with depth will hereinafter be referred to as "stress profiles."

Figure 10 illustrates the effect of the different correction factors on a stress profile produced by glass-bead peening with 60μ beads for 5 seconds. The stress profile after the Lorentz polarization and absorption corrections is shown by the first curve. (Each symbol represents a single stress measurement.) The beam-penetration correction was then applied to yield the second curve. Note that this correction had a very significant effect on the shape of the stress profile in the layers near the surface. The stress in the first layer is reduced, while the stress in the next two or three

layers is substantially increased. As would be expected, the shape of the initial stress profile determines the magnitude and direction of the beam-penetration correction. Finally, the subsurface correction accounts for relaxation effects due to the removal of layers of material and yields the final stress profile as shown by the third curve. This correction tended to reduce the compressive stress at each point. The effect of the subsurface correction is generally small until rather large penetrations are reached (ref. 5).

The stress profiles obtained after various 5-second glass-bead-peening treatments are shown in figure 11. Unlike the results of surface measurements (fig. 4(a)), particle size is now seen to have a strong influence on the magnitude of the stress profile, with the larger particles producing the higher compressive stresses. The stress profiles for the two 30μ glass-bead-peening treatments showed that higher compressive stresses were produced in Ti-8Al-1Mo-1V than Ti-6Al-4V. Note also that all the glass-bead-peened coupons except those treated with 425μ beads exhibited a stress profile in which the maximum stress is slightly below the surface. This shape of stress profile along with the lack of the X-ray beam-penetration correction is the reason the smaller particle-size treatments showed apparently greater surface compressive stresses in figure 4(a).

Stress profiles for coupons with blasting and vibratory treatments are presented in figure 12. Figure 12(a) shows that aluminum oxide blasting treatments with larger particles produced greater compressive stresses. For some reason the 75μ sand-blasting treatment produced a larger depth of compression than treatments with approximately the same size aluminum oxide. Both sand blasting and 70μ aluminum oxide blasting produced stress profiles

in which the maximum stress was slightly beneath the surface. It is interesting to note that this particular shape of stress profile is produced by peening or blasting with particles of 75μ or less.

The stress profiles for Ti-6Al-4V and Ti-8Al-1Mo-1V coupons after vibratory treatments are shown in figure 12(b). The frequency of the vibratory bath was 1375 cpm. Note that these coupons were treated on only one face to simplify analysis and therefore cannot be compared directly with the surface stresses presented in figure 4(c) for coupons treated on both sides. Nevertheless, the stress profiles clearly demonstrate the dependence of residual compressive stress on treatment time. Longer treatment times produce a greater magnitude and depth of compressive stress. The maximum compressive stress created by the vibratory treatment was located slightly below the surface. This characteristic was observed in studies of various tumbling processes on steels (ref. 6) and was believed to be associated with the scratching action of the sharp points of the abrasive. Again, higher compressive stresses were produced in Ti-8Al-1Mo-1V than in Ti-6Al-4V as demonstrated by the two stress profiles produced by a 26-hour treatment. Although the duplicate tests performed on the two titanium alloys are certainly limited, it does appear that the treatments tended to produce higher compressive stresses in Ti-8Al-1Mo-1V. This could be due, in part, to the higher modulus of elasticity and slightly greater sheet thickness of the Ti-8Al-1Mo-1V.

Effect of Surface Treatments on Tensile Properties

The tensile properties of Ti-6Al-4V and Ti-8Al-1Mo-1V before and after various surface treatments are listed in table II. The only treatment which caused noticeable change in tensile properties was glass-bead peening with

425μ beads. This treatment caused a reduction in yield strength of approximately 10 percent in both alloys. The loss in yield strength was accompanied by a decrease in elongation and an increase in ultimate strength. These results can be justified by considering the stress profile for Ti-6Al-4V having the 425μ glass-bead-peening treatment (fig. 11). Under equilibrium conditions, a 6-mil layer under an average compressive stress of 80 ksi would produce approximately a 30-ksi tensile stress across the core of the specimen. Therefore, a superimposed tensile load causes the core to yield before the outer layers at a stress below that for the untreated material. Then, after further load is applied, the large plastic strains alleviate the residual-stress effects and the specimen reaches an ultimate stress which is slightly higher than that for the untreated material due to cold working of the surface layers. The other surface treatments affected such a thin layer of material that residual tensile stresses in the core were quite small. Consequently, any reductions in yield strength were also small.

Stress Relaxation of Residual Stresses

The results of the stress-relaxation tests on Ti-6Al-4V are given in figure 13 where percentage of the residual-surface stress remaining is plotted against temperatures up to 800° F for exposures of 10, 100, and 1000 hours.

Figure 13(a) shows the results for specimens given a 425μ glass-bead-peening treatment which produced an initial surface compressive stress of 115 ksi. Noticeable relaxation was observed at temperatures as low as 400° F with almost complete relaxation after 1000 hours at 800° F. Figure 13(b) presents the results for coupons having a 75μ sand-blasting treatment and an initial compressive stress of 70 ksi. Measurable stress relaxation occurred in these specimens only at 600° F and 800° F. Similar results

were obtained for coupons given a 52-hour vibratory treatment at 1750 cpm (fig. 13(c)). The initial compressive stress created by this treatment was 80 ksi. It should be pointed out that with a high residual-stress level, the lowering of the proportional limit at elevated temperatures may be sufficient to cause a certain amount of immediate stress relief. This process differs from that described for creep or other stress relaxation phenomena which are time dependent. Although no attempts have been made to separate the two processes in these experiments the data at 400° F deserve comment. At 400° F the only stress relaxation that was measured occurred in the glass-bead-peened coupons which exhibited a relatively high surface compressive stress of 115 ksi (fig. 13(a)). Since Ti-6Al-4V shows a reduction of 20 percent in yield strength at 400° F (ref. 7) it is reasonable to assume that the proportional limit is reduced by approximately the same amount or, in this case, to a value of about 100 ksi. Therefore, the stress relaxation measured at 400° F for the glass-bead-peened coupons was probably due entirely to the lowering of the proportional limit. The residual surface compressive stresses produced by sand blasting and the vibratory treatment were not relieved because they were below the proportional limit at 400° F.

In order to determine the applicability of rate parameters for correlation of the relaxation data, the data in figure 13 were plotted using the Larson-Miller time-temperature parameter (ref. 8). The results of this analysis are shown in figure 14 where residual stress is plotted as a function of $T_R(20 + \log t)$; T_R is temperature in degrees Rankine and t is time in hours. Curves for each of the three treatments are faired through the data. Observe that, as temperatures over 400° F are reached, the curves for all three treatments fall into one band. It was therefore concluded that the

residual stress induced by glass-bead peening, blasting, or vibratory tumbling underwent the same rate process for relaxation at elevated temperatures. Furthermore, it seems reasonable that any surface treatment which induces compressive stresses in Ti-6Al-4V would also fall in the same band.

CONCLUDING REMARKS

In this investigation residual stresses created in Ti-6Al-4V and Ti-8Al-1Mo-1V sheet by glass-bead peening, sand or aluminum oxide blasting, and a vibratory tumbling treatment have been measured using an X-ray diffraction technique. The residual compressive stress produced by peening or blasting was increased by increasing the particle size. An increase in treatment time or vibrational frequency increased the compressive stress created by the vibratory treatment. The only treatment that noticeably affected the tensile properties of the titanium alloys was glass-bead peening with the largest bead size which caused a 10-percent reduction in yield strength. Significant stress relaxation occurred in all the treated Ti-6Al-4V coupons exposed at 600° F and 800° F and appeared to be governed by the same rate process.

REFERENCES

1. Almen, J. O.; and Black, P. H.: Residual Stresses and Fatigue in Metals. McGraw-Hill Book Co., Inc., 1963.

2. Heimerl, G. J.; Braski, D. N.; Royster, D. M.; and Dexter, H. B.: Salt Stress Corrosion of Ti-8Al-1Mo-1V Alloy Sheet at Elevated Temperatures. NASA paper presented at Pacific Area Meeting of the ASTM, Oct. 31-Nov. 5, 1965.

3. Pride, Richard A.; and Woodard, John M.: Salt-Stress-Corrosion Cracking of Residually Stressed Ti-8Al-1Mo-1V Brake-Formed Sheet at 550° F (561° K). NASA TM X-1082, 1965.

4. Christensen, A. L., et al.: Measurement of Stress by X-Ray. SAE Inform. Rept. TR-182, 1960.

5. Moore, M. G.; and Evans, W. P.: Mathematical Correction for Stress in Removed Layers in X-Ray Diffraction Residual Stress Analysis. SAE Trans., vol. 66, 1958, p. 340.

6. Letner, H. R.: Stress Effects of Abrasive Tumbling. ASM Transactions, vol. 51, 1959.

7. Weiss, V.; and Sessler, J. G., eds.: Aerospace Structural Metals Handbook. Volume II - Non-Ferrous Alloys. ASD-TDR-63-741, Vol. II, U.S. Air Force, Mar. 1963. (Revised Mar. 1965.)

8. Larson, F. R.; and Miller, James: A Time-Temperature Relationship for Rupture and Creep Stresses. Trans. ASME, vol. 74, no. 5, July 1952, pp. 771-775.

TABLE I.- TREATMENT PARAMETERS

Alloy	Treatment	Commercial designation	Particle composition	Average particle size	Pressure, psi	Nozzle size, in.	Treatment time
Ti-6Al-4V (annealed)	Bead peening	MS-P	Glass	425μ	60	3/16	2, 5, and 10 sec
		MS-L	Glass	60μ	60	3/16	2, 5, and 10 sec
		MS-XL	Glass	30μ	60	3/16	2, 5, and 10 sec
	Blasting	80 grit	Al_2O_3	200μ	50	9/32	5, 15 and 30 sec
		120 grit	Al_2O_3	110μ	50	9/32	5, 15 and 30 sec
		220 grit	Al_2O_3	70μ	50	9/32	5, 15 and 30 sec
		160 grit	SiO_2	75μ	50	9/32	5, 15 and 30 sec
	Vibratory - 1375 cpm		Al_2O_3	5/8-inch triangles, 1/4-inch thick	---	----	13, 26 and 52 hr
	Vibratory - 1750 cpm		Al_2O_3		---	----	13, 26 and 52 hr
Ti-8Al-1Mo-1V	Bead peening	MS-XL	Glass	30μ	60	3/16	2, 5, and 10 sec
	Vibratory - 1375 cpm		Al_2O_3	5/8-inch triangles, 1/4-inch thick	---	----	13, 26 and 52 hr

TABLE II.- TENSILE-TEST RESULTS

(a) Ti-6Al-4V

Surface treatment	Sheet no.	Young's modulus, psi	Yield strength, psi	Ultimate strength, psi	Elongation, percent in gage length	
					1 in.	2 in.
As-received material	1	16.37×10^6	149.2×10^3	163.3×10^3	8	10.5
		16.22	149.8	162.7	8	10
			152.1	162.8	6	10
			153.0	163.2	8	11.5
Glass-bead peened 30μ 15 sec	1		151.1	167.8	7	9.5
			150.3	167.0	6	9
Glass-bead peened 30μ 30 sec	1		156.8	168.0	8	9
			151.1	167.2	5	9
Glass-bead peened 425μ 15 sec	1		135.7	166.0	6	9
			134.5	165.7	8	8.5
Glass-bead peened 425μ 30 sec	1		135.7	166.0	5	8.5
			134.1	165.9	4	8
Al_2O_3 blasting 200μ 15 sec	1		149.2	162.2	4.5	9.5
			149.0	159.5	6	10.5
Al_2O_3 blasting 70μ 15 sec	1		151.3	162.0	5	10
			153.2	164.5	5	9
Sand blasting 75μ 15 sec	1		151.4	165.5	4	9
			151.0	164.0	5	10
Vibratory treatment 26 hr 1375 cpm	1		153.0	163.0	5.5	10
			154.5	164.5	6	10.5
Vibratory treatment 26 hr 1750 cpm	1		155.0	167.1	7	10.5
			155.5	169.0	5	6.5

TABLE II.- TENSILE-TEST RESULTS - Concluded

(b) Ti-8Al-1Mo-1V

Surface treatment	Sheet no.	Young's modulus, psi	Yield strength, psi	Ultimate strength, psi	Elongation, percent in gage length	
					1 in.	2 in.
As-received material	1	18.20×10^6	134.3×10^3	149.1×10^3	8	12.5
		18.12	134.7	149.9	12	13.5
			135.7	149.9	12	13
			133.9	149.7	12	13
Glass-bead peened 30μ 15 sec	1		134.7	150.9	8	12.5
			133.7	151.0	10	12
Glass-bead peened 30μ 30 sec	1		134.7	152.1	12	12.5
			134.2	150.3	8	12
Sand blasting 75μ 15 sec	1		132.0	150.7	8	12
			131.8	150.5	8	11
Vibratory treatment 26 hr 1375 cpm	1		134.2	149.8	8	12
			134.7	150.2	10	13
Vibratory treatment 52 hr 1375 cpm	1		134.4	150.4	10	13
			134.8	150.9	10	13
As-received material	2	17.25	130.0	142.5	8	11
			130.0	143.5	9	11.5
Glass-bead peened 425μ 30 sec	2		114.2	145.0	8	12
			114.8	145.0	8	10

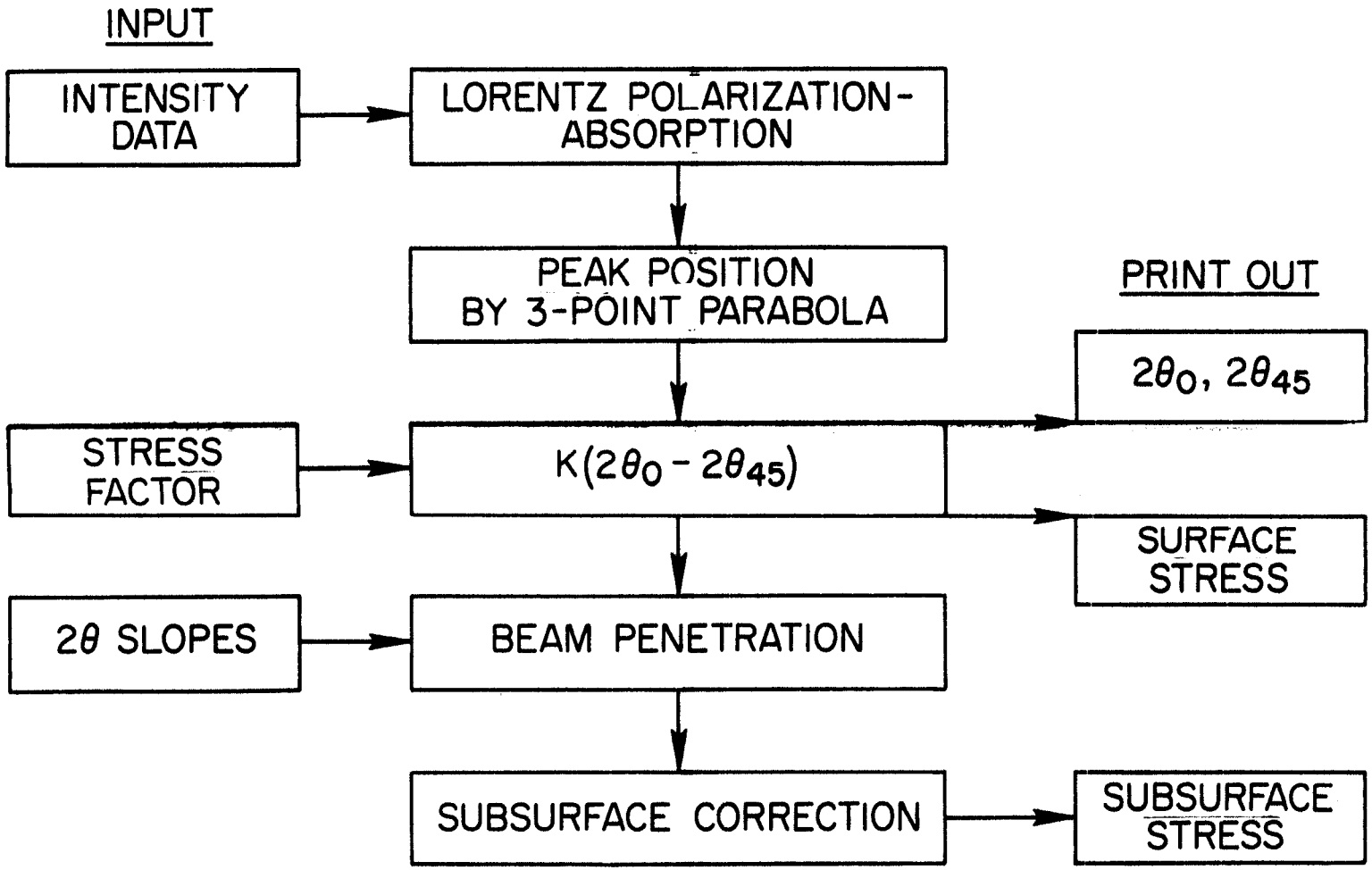

Figure 1.- Schematic of computer program for analysis of X-ray data for stress determination.

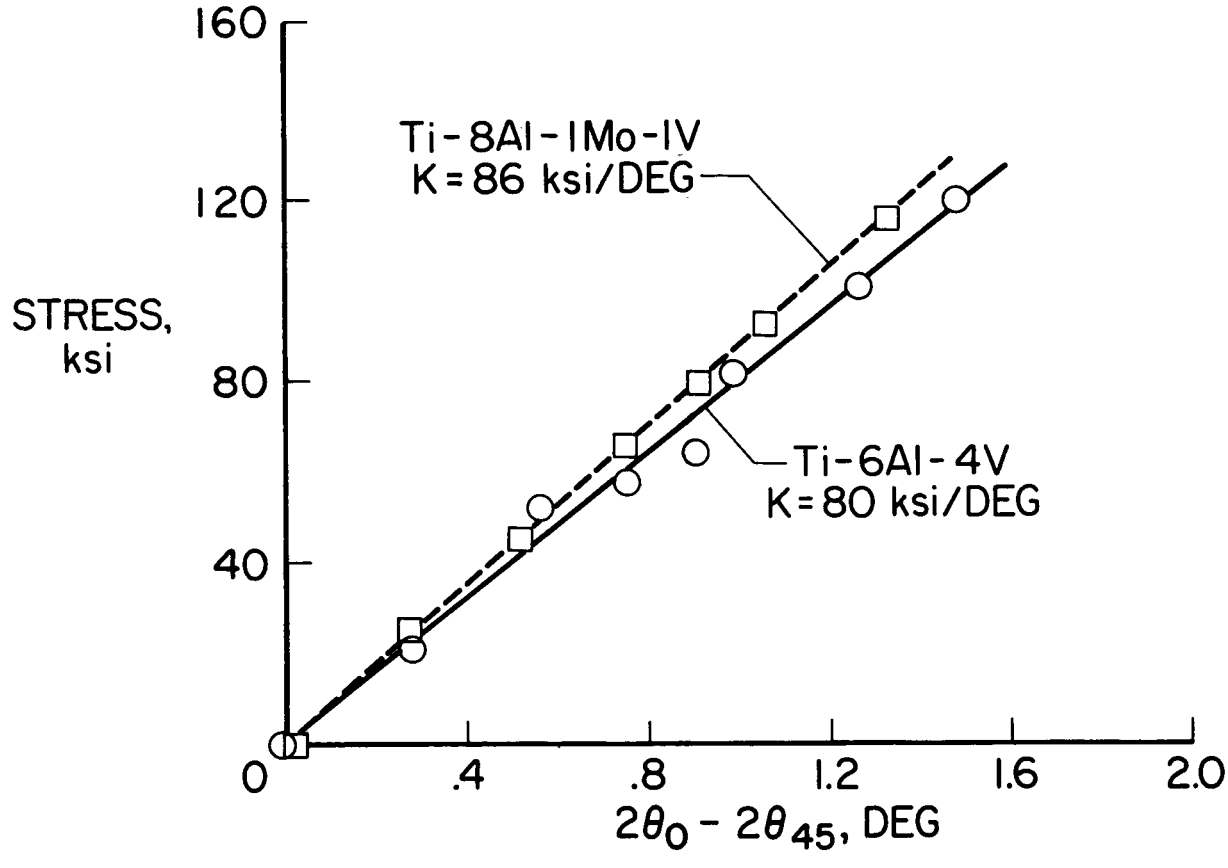

Figure 2.- Stress factor calibration.

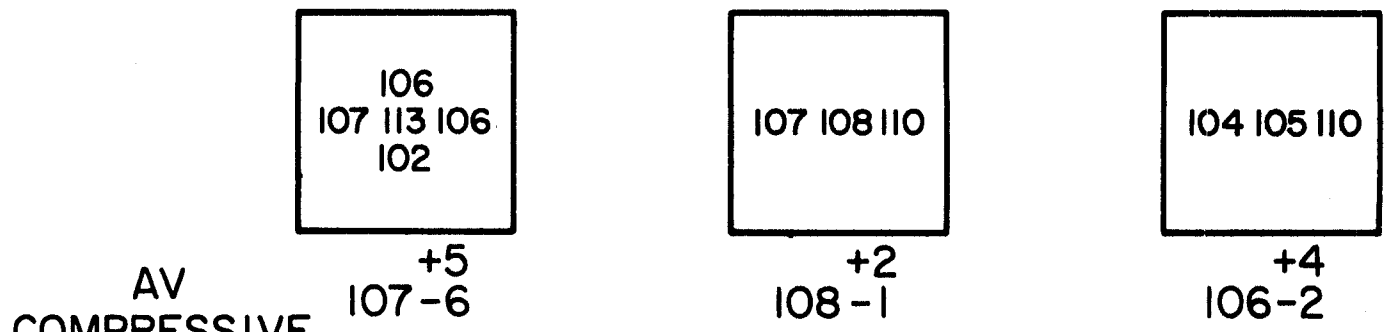

(a) Peening time - 2 sec.

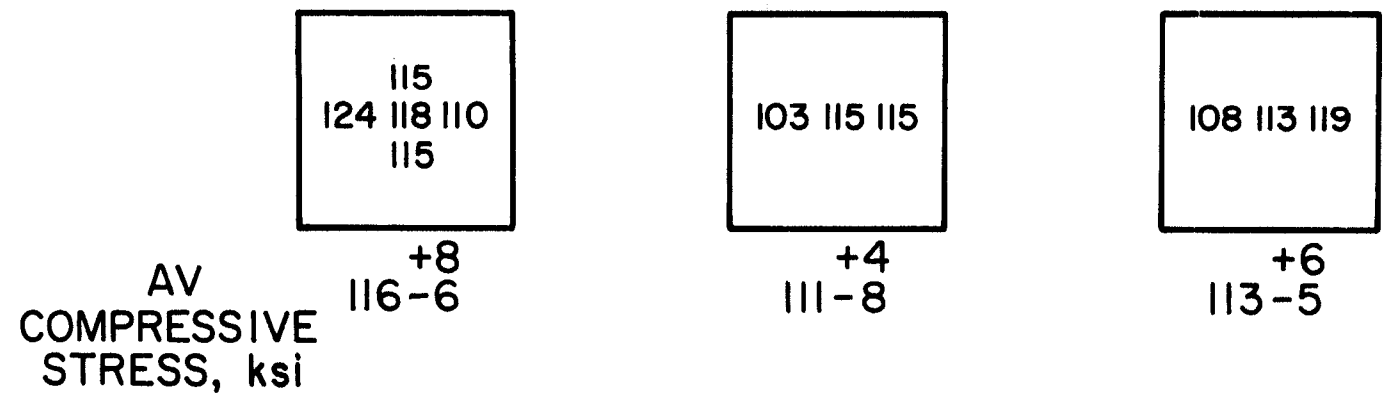

(b) Peening time - 10 sec.

Figure 3.- Variation of residual surface stresses produced by 425μ glass-bead peening of Ti-6Al-4V.

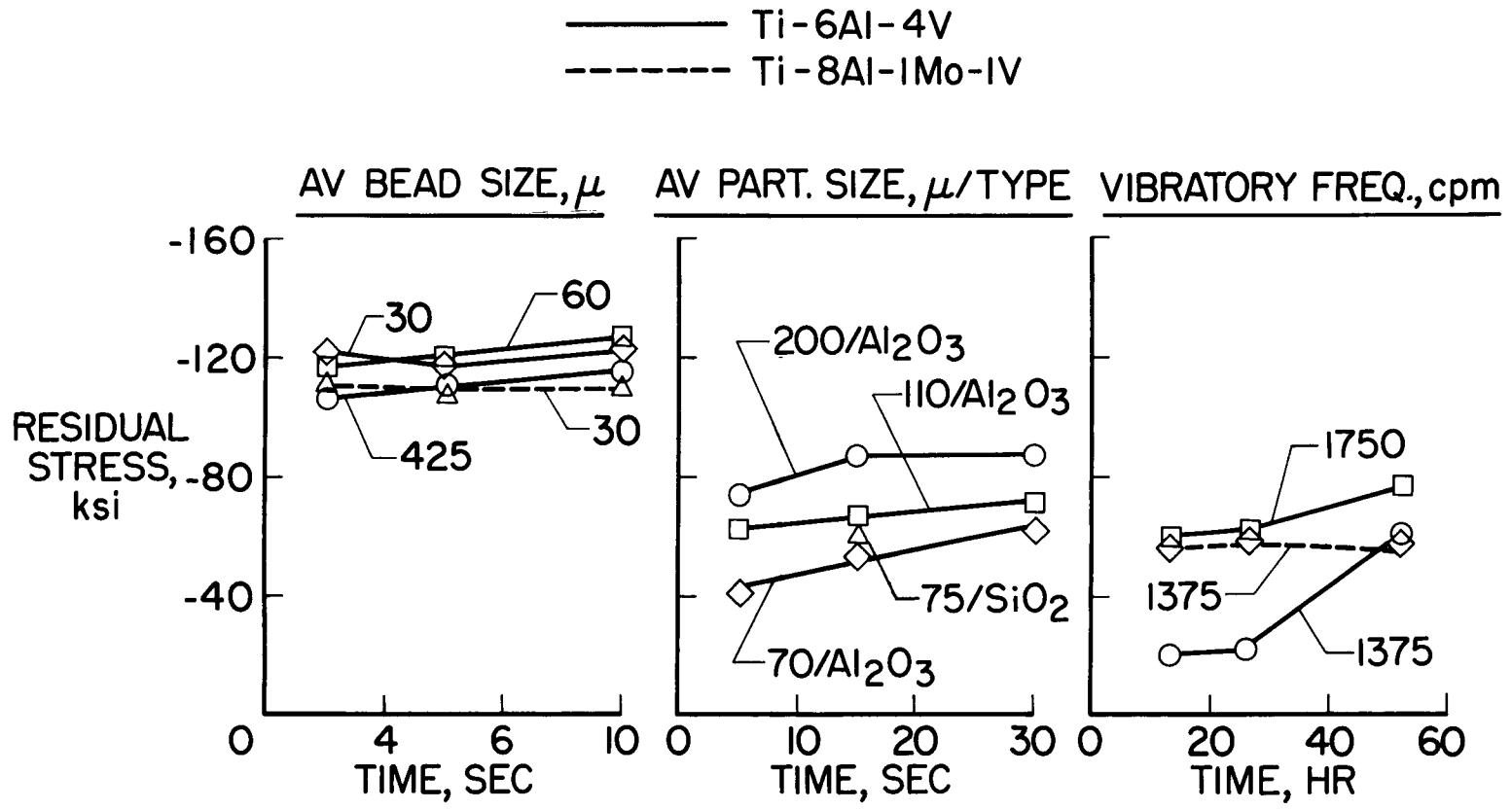

(a) Glass-bead peening.

(b) Sand and aluminum oxide blasting.

(c) Vibratory.

Figure 4.- Effect of treatment time on residual surface stress.

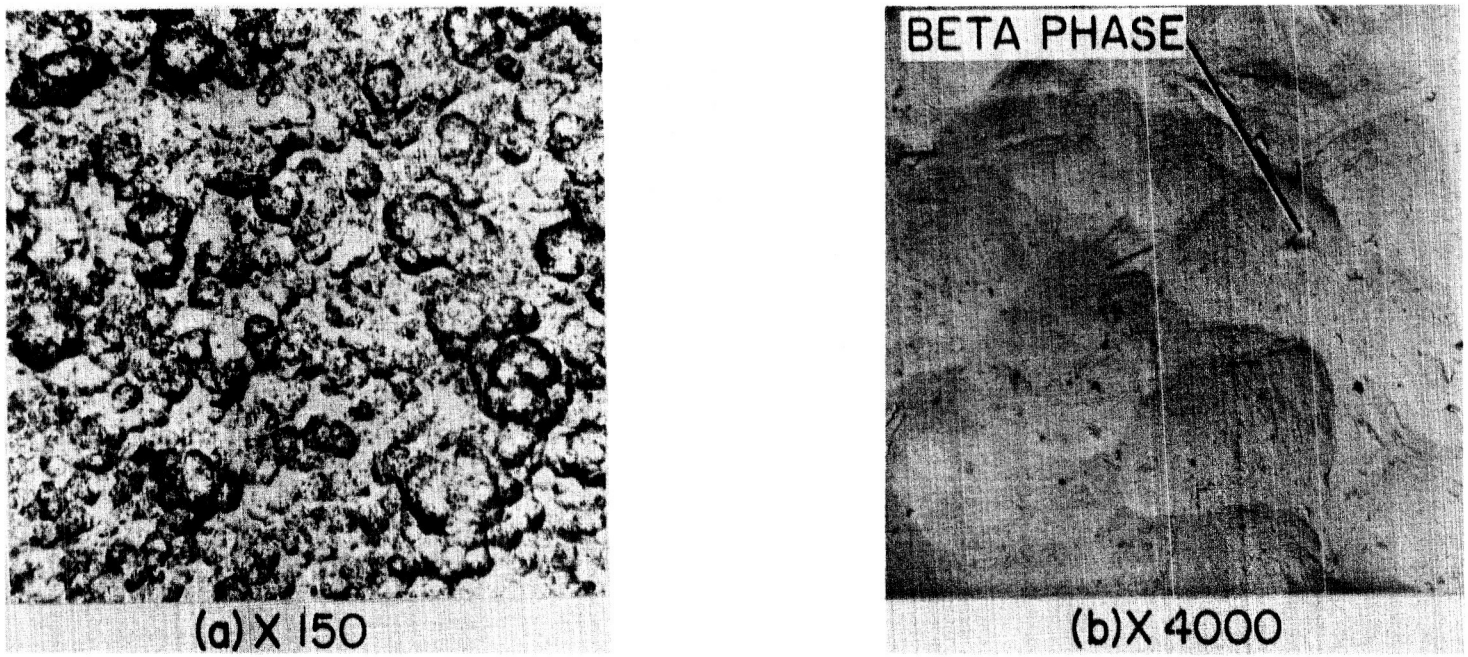

Figure 5.- Light and electron photomicrographs of untreated Ti-6Al-4V coupon surface.

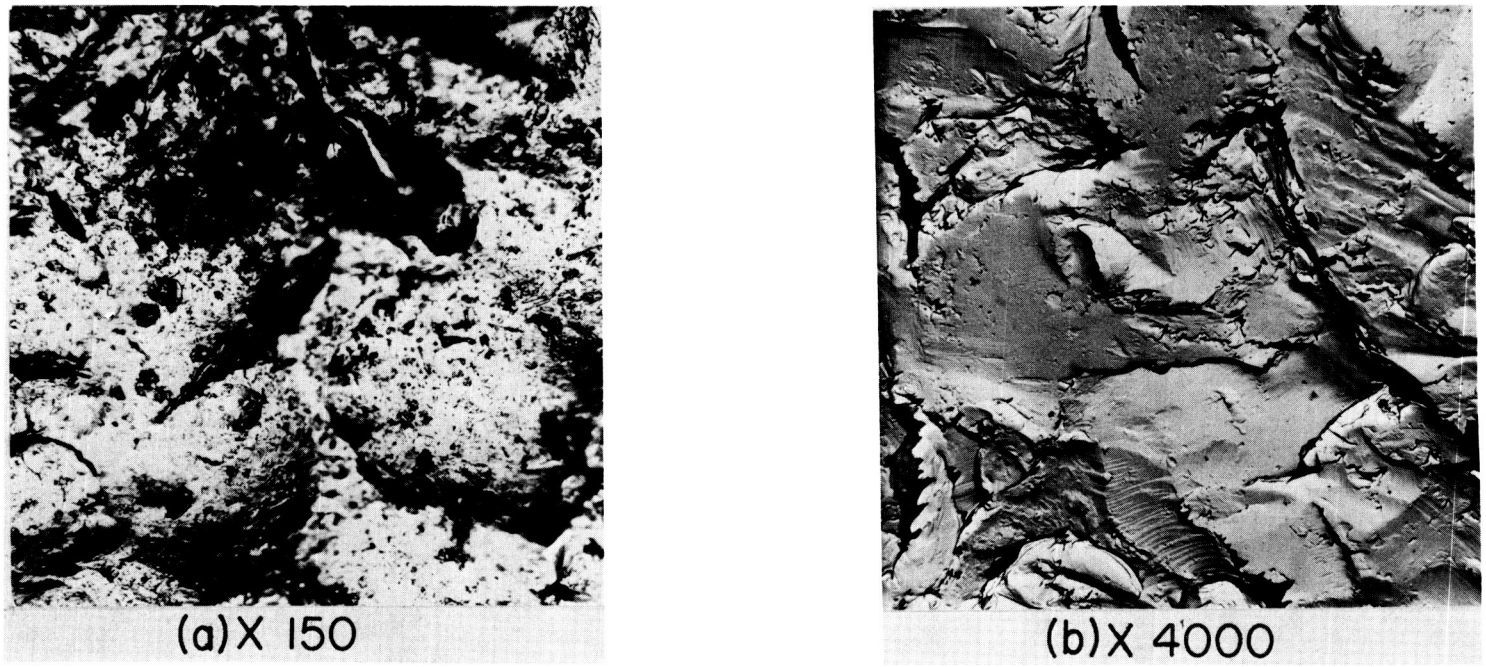

Figure 6.- Light and electron photomicrographs of Ti-6Al-4V coupon surface after 425μ glass-bead peening for 5 seconds.

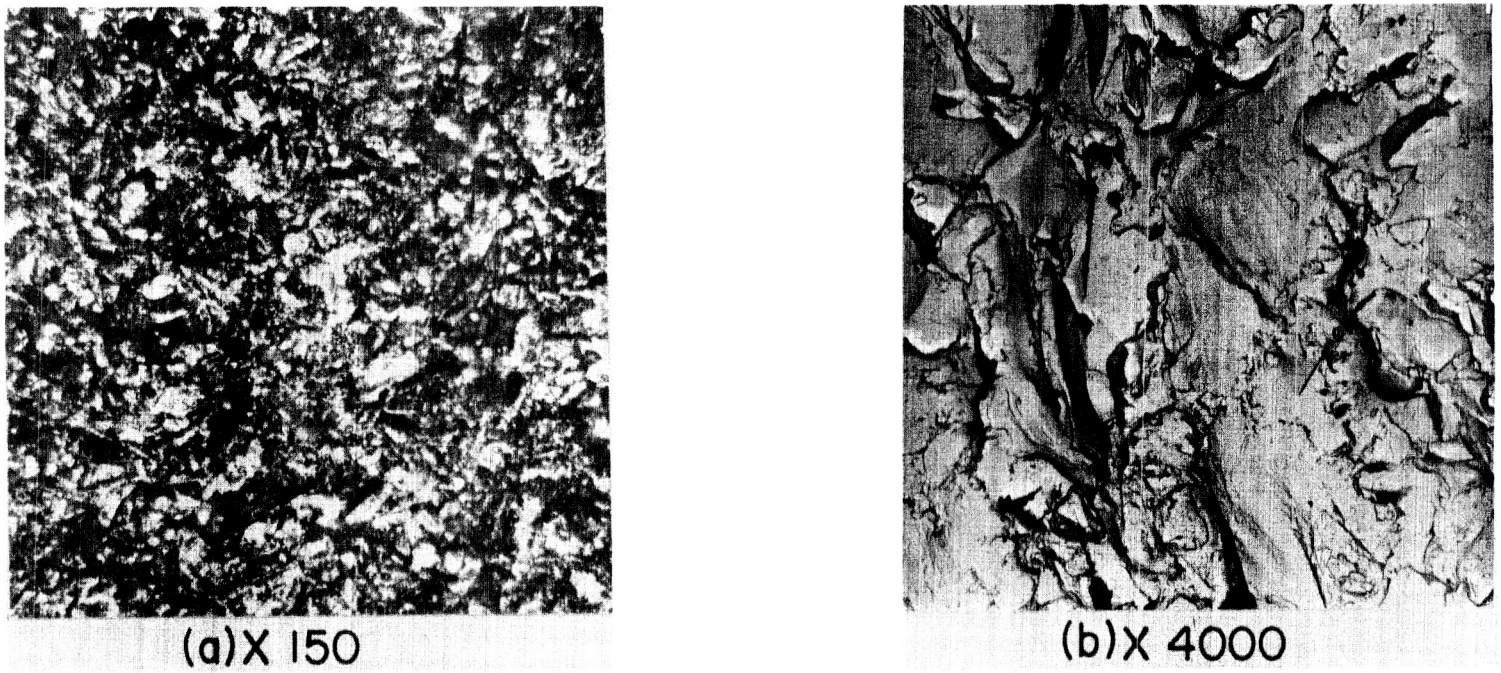

Figure 7.- Light and electron photomicrographs of Ti-6Al-4V coupon surface after blasting with 200μ aluminum oxide for 15 seconds.

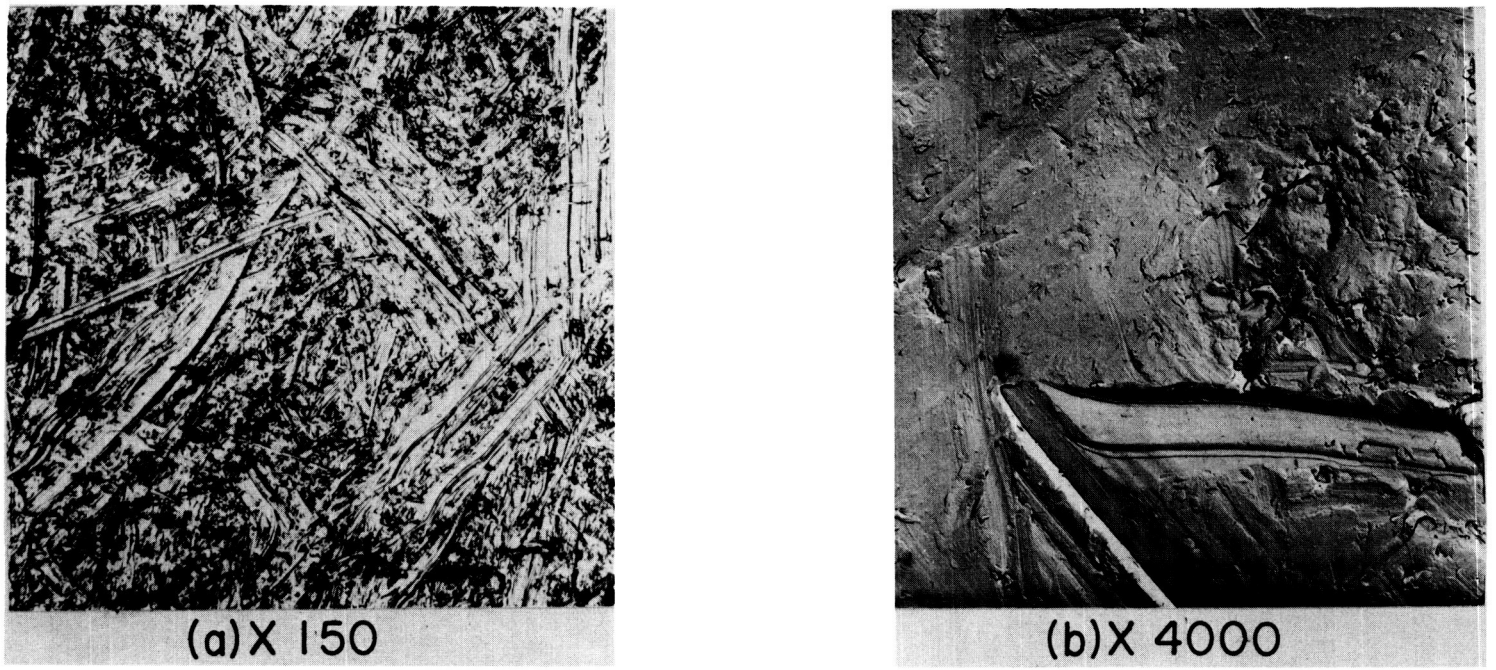

Figure 8.- Light and electron photomicrographs of Ti-6Al-4V coupon surface after a 26-hour vibratory treatment at 1375 cpm.

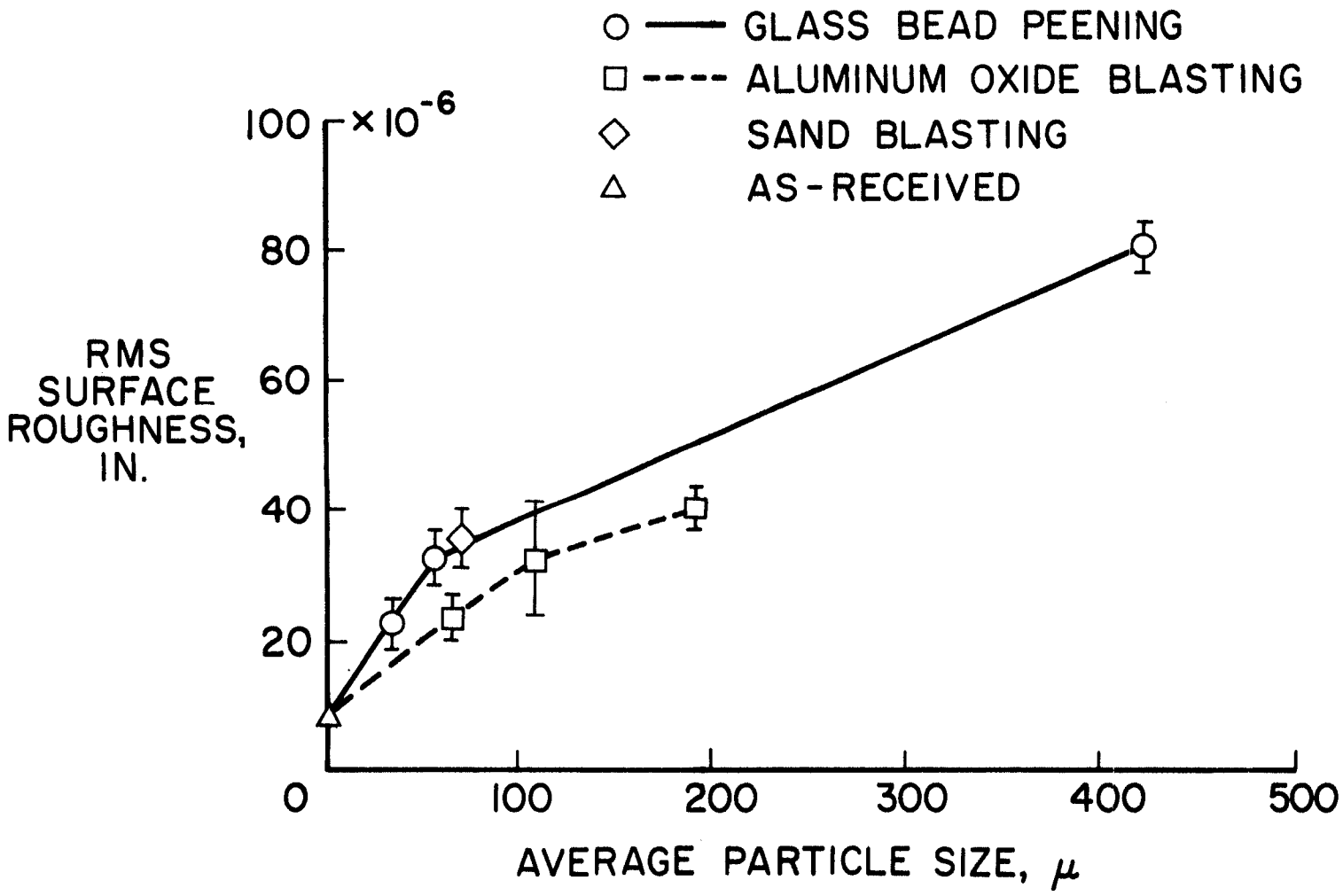

Figure 9.- Surface roughness measurements on treated Ti-6Al-4V sheet.

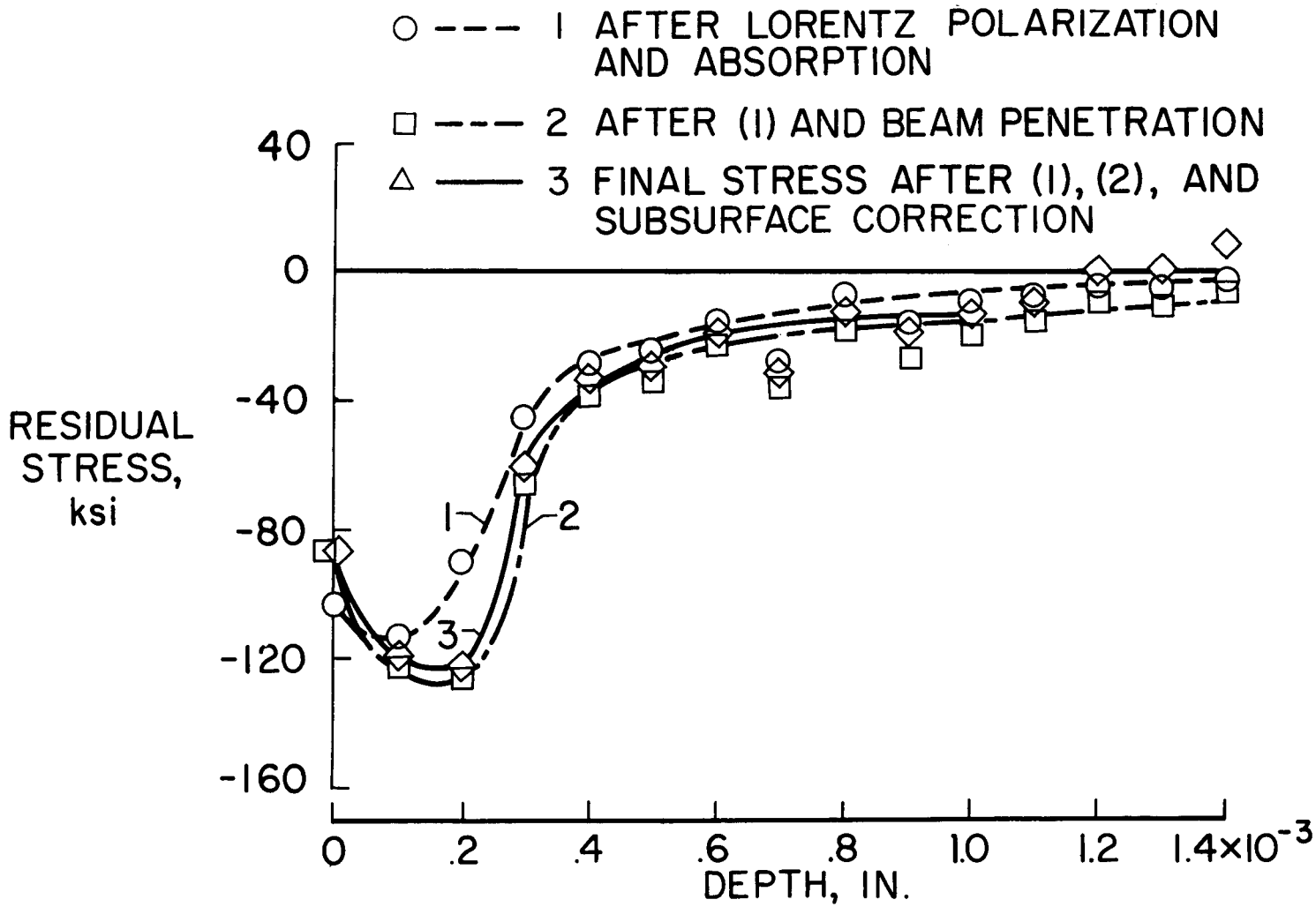

Figure 10.- Effect of correction factors on stress profile for Ti-6Al-4V with a 5 sec, 60μ glass-bead peening treatment.

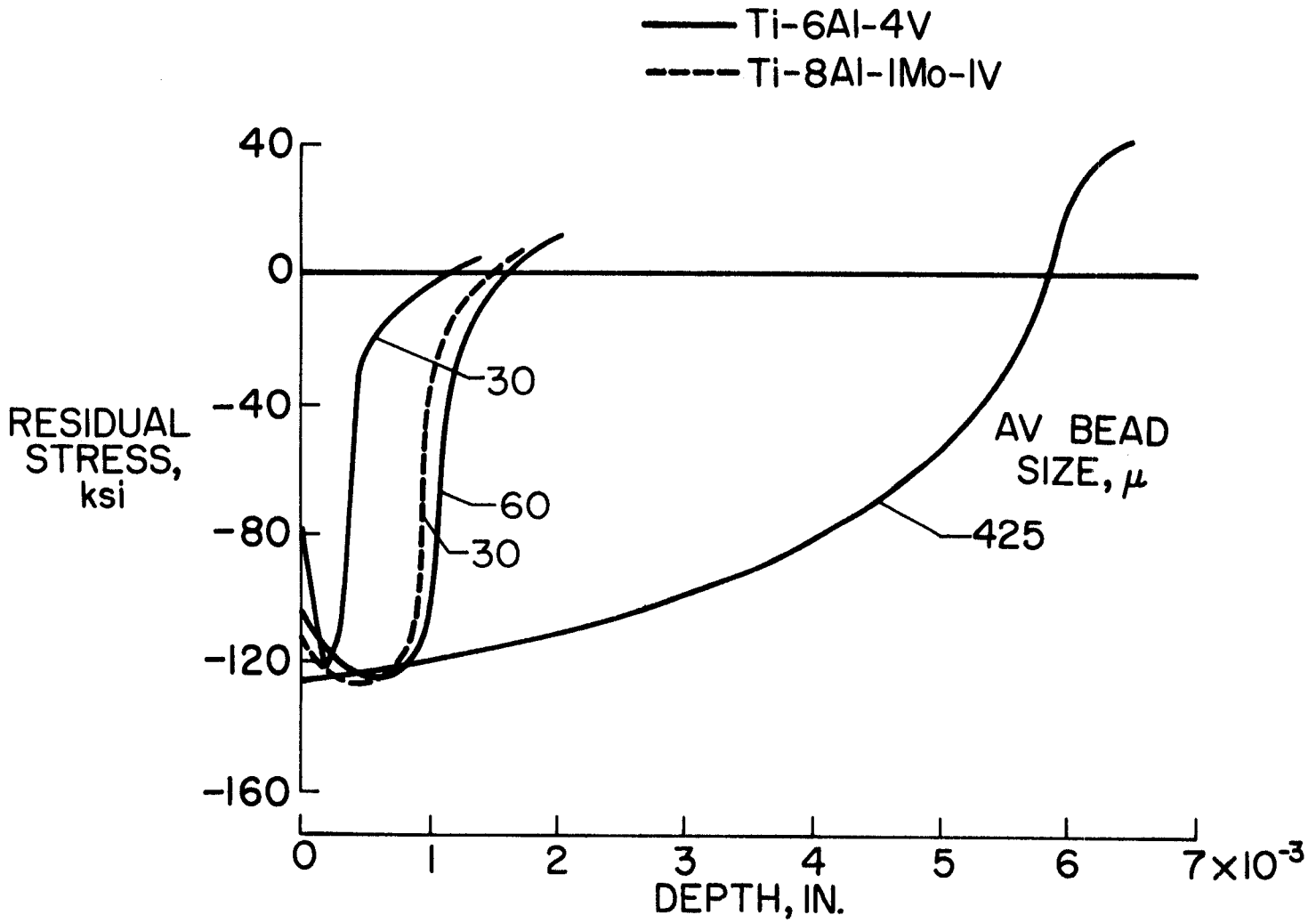

Figure 11.- Stress profiles produced by glass-bead peening for 5 seconds.

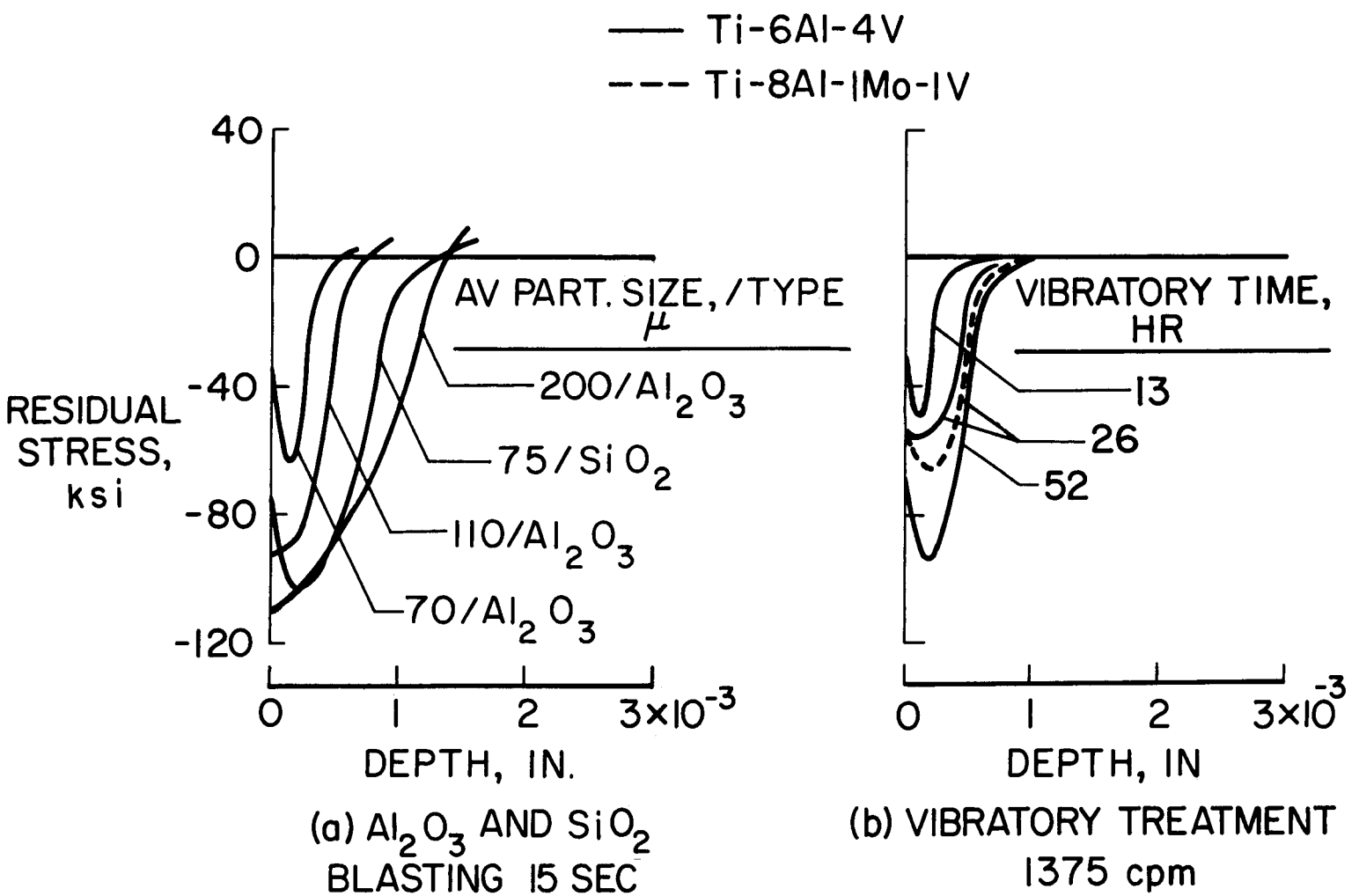

Figure 12.- Stress profiles produced by blasting and vibratory treatments.

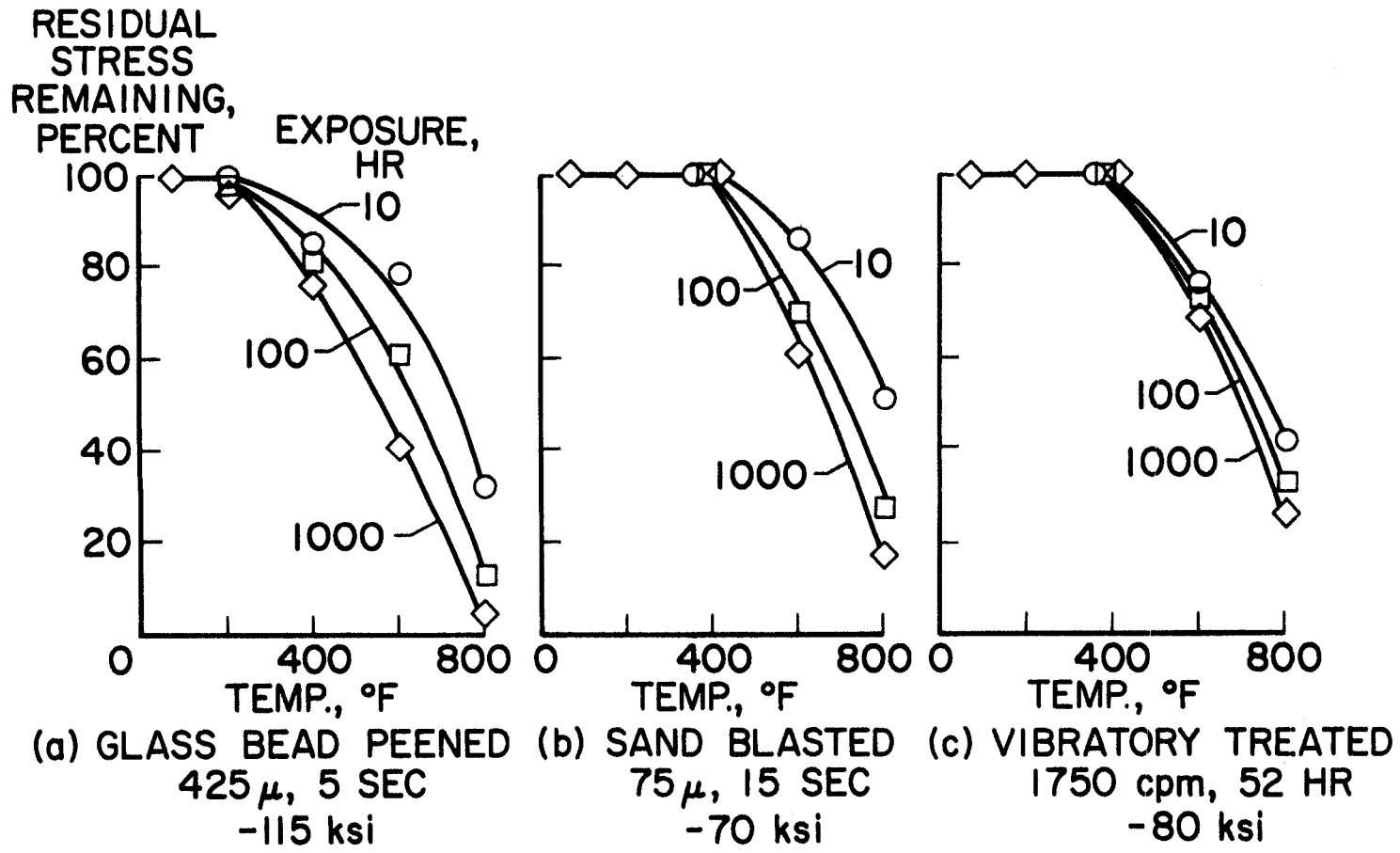

Figure 13.- Stress relaxation in Ti-6Al-4V after various surface treatments.

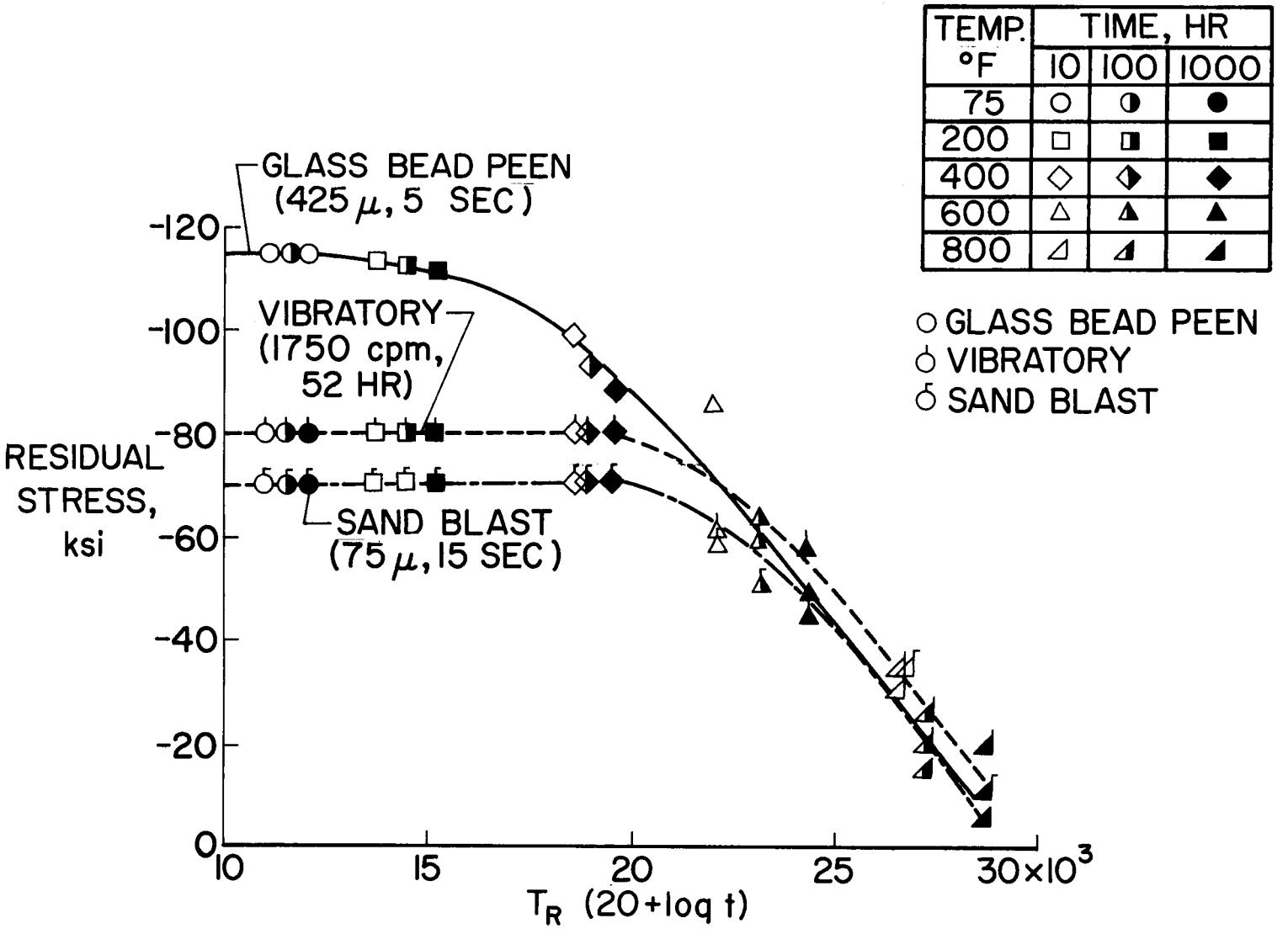

Figure 14.- Application of Larson-Miller parameter to stress relaxation data.